Effect of *p*H on the structure of lipoplexes

Giulio Caracciolo,[1,a)] Daniela Pozzi,[1] Ruggero Caminiti,[1] Cristina Marchini,[2] Maura Montani,[2] and Heinz Amenitsch[3]
[1]*Department of Chemistry, University of Rome "La Sapienza," Piazzale Aldo Moro 5, 00185 Rome, Italy*
[2]*Genetic Immunization Laboratory, Department of Molecular Cellular and Animal Biology, University of Camerino, Via Gentile III da Varano, 62032 Camerino (MC), Italy*
[3]*Institute of Biophysics and Nanosystems Research, Austrian Academy of Sciences, Schmiedelstrasse 6, A-8042 Graz, Austria*

(Received 4 March 2008; accepted 22 April 2008; published online 7 July 2008)

Recently, it has been postulated that a primary importance of the *p*H is for accomplishing efficient lipid-mediated translocation of nucleic acids across the endosomal membrane into the cytosol for transport to the nucleus. With the aim of providing insight into the postulated correlation between transfection efficiency, phase evolution of lipoplexes upon acidification, and DNA release, we investigated the *p*H dependence of the structure of low efficiency 1,2-dioleoyl-3-trimethylammonium-propane-dioleoylphosphocholine/DNA and high efficiency 3β-[*N*-(*N*′,*N*′-dimethylaminoethane)-carbamoyl]-cholesterol-dioleoylphosphatidylethanolamine/DNAlipoplexes by high-resolution synchrotron small-angle x-ray diffraction, while the extent of DNA release was estimated by means of electrophoresis on agarose gels. Here we show that upon acidification from physiological to acidic values (as those characteristic of endosomes), (i) the lamellar structure of lipoplexes was preserved with a decrease in the one-dimensional DNA packing density, reflecting a *p*H-induced contraction of interfacial area of lipid head groups and (ii) DNA was not released from lipoplexes. Distinct levels of transfection between lipoplexes were interpreted in terms of the different DNA-binding capacities of cationic liposomes. © *2008 American Institute of Physics*. [DOI: 10.1063/1.2949705]

I. INTRODUCTION

At present, there is a high level of interest in complexes consisting of DNA mixed with cationic liposomes (CLs).[1–3] This extraordinary interest arises because the complexes mimic natural viruses as carriers of DNA into cells in worldwide human gene therapy clinical trials. Mixing CLs and DNA results in their spontaneous self-assembling into highly organized liquid crystalline complexes (lipoplexes). For transfection purposes, positively charged lipoplexes are used as they bind electrostatically to the negatively charged cell surface proteoglycans with sulfated groups.[4–6]

Synchrotron x-ray diffraction experiments have been used to solve the structure at the angstrom scale. Three types of structures have been observed.[7–10] These include a multilamellar structure with DNA monolayers sandwiched between cationic membranes (L_{α}^{C} phase),[7,8] an inverted hexagonal H_{II}^{C} phase comprised of lipid-coated DNA strands arranged on a hexagonal lattice, and a lattice structure,[9] termed H_{I}^{C}, composed of lipid micelles surrounded by DNA strands forming a three-dimensional substructrure.[10]

Formulations based on the exclusive use of zwitterionic lipids have also been investigated with divalent electrolyte counterions common in biological cells (Mn^{2+}, Ca^{2+}, Co^{2+}, Mg^{2+}, and Fe^{2+}) serving as DNA condensing agents.[11,12] In these complexes, transbilayer DNA ordering has been observed.[13]

Even though some earlier studies suggested superiority in transfection of hexagonal lipoplexes with respect to lamellar ones,[8] experimental evidence invalidated a correlation between structure and activity.[14–16]

However, to meet therapeutic requirements, the efficacy of lipoplexes needs major improvement, and a detailed comprehension of the mechanism of entry in relation to eventual transfection efficiency (TE) could be part of such a strategy. Endocytosis is recognized as the major pathway of entry. After internalization via endocytosis, the internalized complexes exist in endosomes with no virtual access to the cytosol or the nucleus. Endosomes either fuse with lysosomes for degradation or recycle their content back to the cell surface. Unfortunately, lipoplexes lack a protein machinery to destabilize the endosomal membrane. Therefore, the escape of DNA from endosomal compartments is thought to represent a critical barrier to lipoplex-mediated transfection.[17–20]

Recently, it has been postulated that a primary importance of the *p*H is for accomplishing efficient translocation of nucleic acids across the endosomal membrane into the cytosol. Lipids that form a stable bilayer at physiological *p*H$\sim$7 can undergo, at an acidic *p*H, a transition from a bilayer to an inverted hexagonal structure, which fuses and destabilizes the endosomal membrane.[21–24] Such an interaction between the nonlamellar lipoplex structure and the endosomal membrane may promote gene translocation. As a result, the ability of specific lipid species (such as the widely used dioleoylphosphatidylethanolamine) to promote, when protonated, lamellar-to-nonlamellar phase transitions may be a key parameter for DNA transfection. However, unambigu-

[a)]Author to whom correspondence should be addressed. Electronic mail: g.caracciolo@caspur.it.

ous evidences of a correlation between successful formation of nonlamellar phases, DNA release, and efficient transfection are still largely lacking.

In the present study, we employed 1,2-dioleoyl-3-trimethylammonium-propane- dioleoylphosphocholine/DNA (DOTAP-DOPC/DNA) and 3β-[*N*-(*N*′,*N*′-dimethylamino-ethane)-carbamoyl]- cholesterol- dioleoylphosphatidylethanolamine/DNA (DC-Chol-DOPE/DNA) lipoplexes. Such lipid formulations, largely used for gene delivery *in vitro* and *in vivo*, exhibited very different levels of transfection in mouse fibroblast NIH 3T3, ovarian CHO, and tumoral myofibroblastlike A17 cells. With the aim of providing insight into the postulated correlation between TE, the phase evolution of lipoplexes upon acidification, and the DNA release, we investigated the *p*H dependence of the lipoplex structure by high-resolution synchrotron small-angle x-ray diffraction (SAXD), and we estimated the extent of DNA release by means of electrophoresis on agarose gels. Here we show that upon acidification from physiological to acidic values (as those characteristic of endosomes), (i) the lamellar structure of lipoplexes was preserved with a decrease in the one-dimensional (1D) DNA packing density, reflecting a *p*H-induced contraction of the interfacial area of lipid head groups, and (ii) DNA was not released from lipoplexes. Distinct levels of transfection between DOTAP-DOPC/DNA and DC-Chol-DOPE/DNA lipoplexes were interpreted in terms of the different DNA-binding capacities of cationic liposomes.

II. MATERIALS AND METHODS

A. Lipoplexes preparation

Cationic DOTAP and DC-Chol, and neutral DOPE and DOPC were purchased from Avanti Polar Lipids (Alabaster, AL) and used without further purification (Fig. 1, top panel). DOTAP-DOPC and DC-Chol-DOPE CLs were routinely prepared.[14] In brief, each binary mixture, at a molar ratio of neutral lipid in the bilayer Φ=(neutral lipid)/(total lipid) (mol/mol)=0.5, was dissolved in chloroform, and the solvent was evaporated in vacuum for 24 h. The obtained lipid films were hydrated with the appropriate amount of tris-HCl buffer solution (10 mM, *p*H 7.4) to achieve the desired final concentration (~25 mg/ml for x-ray samples). The solutions were incubated at 30 °C for 6 h to allow for the formation of CLs. The obtained liposome solutions were then stored at 30 °C for 24 h to achieve full hydration.[25]

Calf thymus Na-DNA was purchased from Sigma (St. Louis, MO). DNA was dissolved in tris-HCl buffer and was sonicated for 5 min, inducing DNA fragmentation with a length distribution between 500 and 1000 base pairs, which was determined by gel electrophoresis.[6] Lipoplexes were prepared by mixing 100 μl of calf thymus DNA at 5.3 mg/ml with suitable volumes of liposome dispersions. All samples were prepared with the same cationic lipid/DNA ratio (mol/mol), i.e., ρ={[cationic lipid(mole)]/(DNA base)}=2. After storage for 3 days at 4 °C, allowing the samples to reach equilibrium,[25] they were transferred to 1.5-mm-diameter quartz x-ray capillaries (Hilgenberg, Malsfeld, Germany). The capillaries were centrifuged for 5 min at 6000 rpm at room temperature (RT) to consolidate the samples.

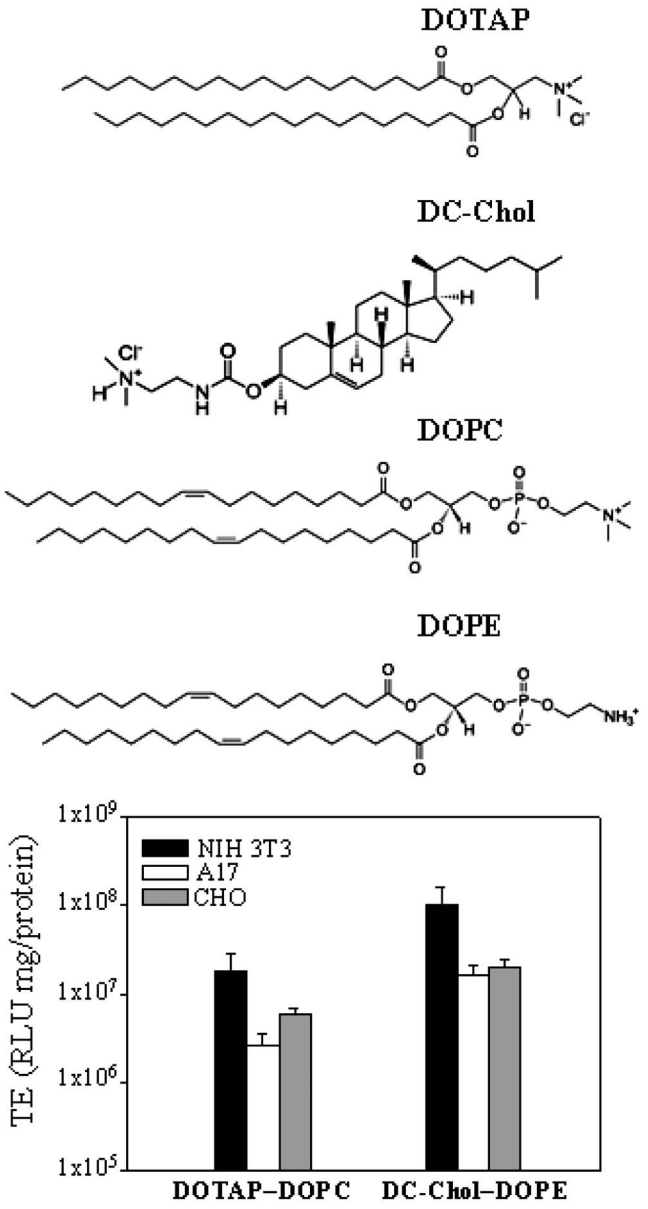

FIG. 1. On the top: chemical structure of the lipids used. On the bottom: TE of DOTAP-DOPC/DNA and DC-Chol-DOPE/DNA lipoplexes in mouse fibroblast (NIH 3T3; black), tumoral myofibroblastlike (A17; white), and ovarian (CHO; gray) cell lines. In both the cell lines, TE of DC-Chol-DOPE/DNA lipoplexes is about one order of magnitude higher than that of the DOTAP-DOPC/DNA ones.

The *p*H was reduced by sequential addition of 10 mM HCl in ~100 μl aliquots and was constantly monitored.

B. Transfection efficiency experiments

Cell lines were cultured in Dulbecco's modified Eagle's medium (DMEM) (Invitrogen, Carlsbad, CA) supplemented with 1% penicillin-streptomycin (Invitrogen) and 10% fetal bovine serum (FBS) (Invitrogen) at 37 °C and 5% CO_2 atmosphere, splitting the cells every 2–4 days to maintain monolayer coverage.

For luminescence analysis, mouse fibroblast NIH 3T3, ovarian CHO, and tumoral myofibroblastlike A17 cells were transfected with pGL3 control plasmid (Promega). The day before transfection, cells were seeded in 24 well plates (150 000 cells/well) using a medium without antibiotics. Cells were incubated until they were 75%–80% confluent, which generally took 18–24 h. For TE experiments, lipoplexes were prepared in Optimem (Invitrogen) by mixing for each well of 24 well plates 0.5 μg of plasmid with 5 μl of sonicated lipid dispersions (1 mg/ml). These complexes were left for 20 min at RT before adding them to the cells. The cells were incubated with lipoplexes in Optimem (Invitrogen) for 6 h to permit transient transfection; the medium was then replaced with DMEM supplemented with FBS. Luciferase expression was analyzed after 48 h and measured with the luciferase assay system from Promega, and light output readings were performed on a Berthold AutoLumat luminometer LB-953 (Berthold, Bad Wildbad, Germany). TE was normalized to milligrams of total cellular protein in the lysates using the Bio-Rad protein assay dye reagent (Bio-Rad, Hercules, CA).

C. Synchrotron small-angle x-ray diffraction measurements

All SAXD measurements were performed at the Austrian SAXS station of the synchrotron light source ELETTRA (Trieste, Italy).[26] SAXD patterns were recorded with a gas detector based on the delay line principle covering a q range of between 0.05 and 1.5 $Å^{-1}$. The angular calibration of the detector was performed with silver behenate [CH3(CH2)20-COOAg] whose d value corresponds to 58.38 Å. Exposure times for every sample were 100 s. No evidence of sample degradation due to radiation damage was observed in any of the samples at this exposure. The data have been normalized for primary beam intensity and detector efficiency as well as having the background subtracted. Temperature was controlled in the vicinity of the capillary to within 0.1 °C (Anton Paar, Graz, Austria).

D. Agarose gel electrophoresis experiments

Electrophoresis studies were conducted on 1% agarose gels containing tris-borate-ethylenediaminetetraacetic acid (EDTA) buffer. After electrophoresis, ethidium bromide (Et-Br) was added and then visualized. Lipoplexes were prepared by mixing 40 μl of lipid dispersions (1 mg/ml, tris-HCl buffer) with 4 μg of pGL3 control plasmid (ρ=2). These complexes were let to equilibrate for 1 h at RT. The pH was reduced by sequential addition of 10 mM HCl in 5–10 μl aliquots and was continuously monitored. Then, 10 μl of each sample were mixed with 2 μl of loading buffer (glycerol, 30% v/v; bromophenol blue, 0.25% v/v) and subjected to agarose gel electrophoresis for 1 h at 80 V. The electrophoresis gel was visualized and digitally photographed using Kodak Image Station, model 2000 R (Kodak, Rochester, NY).

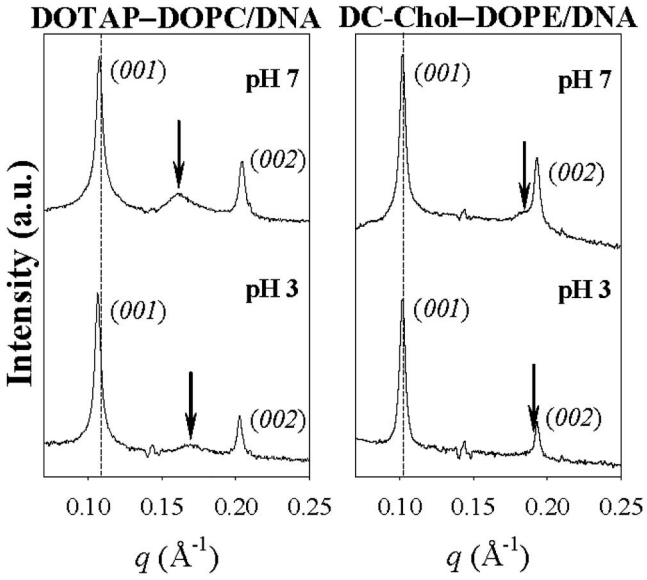

FIG. 2. SAXD patterns of DOTAP-DOPC/DNA (left panel) and DC-Chol-DOPE/DNA (right panel) at two different pH values: pH 7 and pH 3. As pH decreases, DNA peak (marked by arrows) shifted to higher q values (i.e., shortest DNA spacings) as a result of the lateral expansion of the lipid headgroups. Vertical dashed line identifies the position of the (001) Bragg peak at pH 7.

III. RESULTS

A. Transfection efficiency results

In Fig. 1 (bottom panel), TE of DOTAP-DOPC/DNA and DC-Chol-DOPE/DNA lipoplexes in mouse fibroblast NIH 3T3, tumoral myofibroblastlike A17, and ovarian CHO cell lines is reported. The same dependency of TE against lipoplex formulations was found for all cell lines. Indeed, for all cell lines, TE of DC-Chol-DOPE/DNA lipoplexes was about one order of magnitude higher than that of DOTAP-DOPC/DNA ones. According to literature, TE was also found to be dependent on the given cell line. The NIH 3T3 cell line is much more easily transfected than A17 ones, while intermediate levels of transfection were obtained with CHO cells.

In principle, the observed differences in TE between DOTAP-DOPC/DNA and DC-Chol-DOPE/DNA lipoplexes may be due to a different phase behavior in the endosomal pH range. To further investigate the correlation between TE and pH-induced structural changes in lipoplexes, we performed SAXD measurements on DOTAP-DOPC/DNA and DC-Chol-DOPE/DNA lipoplexes upon acidification.

B. Effect of *p*H on the structure of lipoplexes

Figure 2 shows the SAXD patterns of DOTAP-DOPC/DNA (left panel) and DC-Chol-DOPE/DNA (right panel) systems at two different pH values: pH 7 and pH 3. At pH 7, lipoplexes form highly organized lamellar phases (L_α^C phase). The sharp periodically spaced peaks at q_{00l} are caused by alternating lipid bilayer-DNA-monolayer structure with periodicity $d=2\pi/q_{001}$. The much broader peak (marked by an arrow) is the "DNA peak" arising from the 1D in plane lattice with repeat distance $d_{\mathrm{DNA}}=2\pi/q_{\mathrm{DNA}}$.

Upon lowering the *p*H from *p*H 7 to *p*H 3, SAXD patterns of lipoplexes changed, but the lamellar structure of lipoplexes is essentially preserved with DNA remaining tightly bound to lipid bilayers. In the case of DOTAP-DOPC/DNA lipoplexes (Fig. 2, left panel) the diffraction peaks moved to lower q values as a function of decreasing *p*H, with the lamellar repeat distance d moving from 58.2 to 59.3 Å. It means that lowering the *p*H induces a slight swelling of DOTAP-DOPC membranes, and that electrostatic modifications in membrane charge density do not extend very far into the hydrophobic region of the bilayer.[27]

Even though the variation in the surface polarity arising from changing the bulk *p*H value can dramatically alter the membrane structural and phase behavior, our findings show that the presence of DNA molecules embedded between opposing membranes largely reduces this effect. A direct comparison of the diffraction patterns shows that lowering the *p*H induced simultaneous decrease in height and progressive broadening of diffraction peaks. From a structural point of view, it means that the long-range order along the normal to the lipid bilayer decreases, and the "second-order disorder" in the crystal lattice increases with decreasing *p*H. Such a stacking disorder accounts for the presence of random variations in the bilayer separations.[28]

Similar findings were obtained with DC-Chol-DOPE/DNA complexes (Fig. 2, right panel), the main difference being that the swelling of the lamellar phase was not observed.

Figure 2 also shows that the interhelical DNA-DNA peak shifted to higher q values with decreasing *p*H. In Fig. 3 [panel (a)] we report the DNA repeat distance d_{DNA} as a function of *p*H for DOTAP-DOPC/DNA lipoplexes. Upon gradual acidification, the inter-DNA distance becomes shorter. In a recent publication dealing with the thermotropic behavior of lipoplexes, we have shown that the variation in DNA-DNA spacing is regulated by the lateral expansion of the interfacial area of lipid headgroups, A.[25] Panel (b) of Fig. 3 shows the *p*H dependence of the average interfacial area A per lipid molecule, calculated according to Ref. 29. Such a calculation confirms that the larger distance between DNA strands in DOTAP-DOPC/DNA lipoplexes at *p*H 7 is simply ruled by a larger average interfacial area per lipid molecule.

Interestingly, very similar results were obtained in an independent experiment performed on the DC-Chol-DOPE/DNA system (Fig. 4).

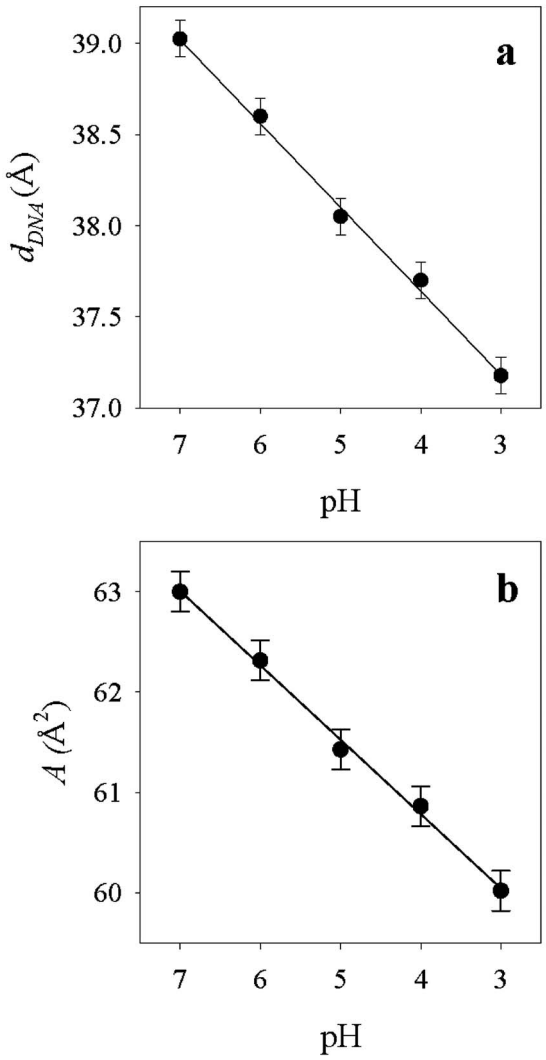

FIG. 3. Panel (a): DNA interdistance d_{DNA} as a function of *p*H for DOTAP-DOPC/DNA lipoplexes. Panel (b): *p*H dependence of the average interfacial area A per lipid molecule of DOTAP-DOPC membranes. Solid lines are the best linear fits to the data.

C. Effect of *p*H on the DNA release

The extent of DNA release from DOTAP-DOPC/DNA and DC-Chol-DOPE/DNA lipoplexes as a function of *p*H was investigated by electrophoresis on agarose gel that allows to determine how much DNA is completely free from lipid.

In Fig. 5, we report the digital photograph of DOTAP-DOPC/DNA and DC-Chol-DOPE/DNA lipoplexes (ρ=2) at decreasing *p*H values. Lane 1 is the control DNA, the high-mobility band was attributed to the most compact (supercoiled) form, and the less-intense one was considered to be the nonsupercoil content in the plasmid preparation.

At *p*H 7, the intensity of free DNA bands varied significantly with lipid formulations. As can be seen in Fig. 5, free DNA is largely present in the DOTAP-DOPC/DNA formulation (lane 2), while DC-Chol-DOPE/DNA binds DNA completely (lane 6).

This finding means that, at a given cationic lipid/DNA molar ratio, the DNA-binding capacity strictly depends on the employed lipid formulation.

Upon acidification, the intensity of the free DNA bands of DOTAP-DOPC/DNA lipoplexes (lanes 2–5) remained roughly the same, while DNA was not released from DC-Chol-DOPE/DNA complexes. These findings indicate that (i) acidification of lipoplexes does not necessarily involve the dissociation and release of DNA from the cationic lipids and (ii) the topology of free DNA is not modified by a drop in *p*H. The latter observation is of primary significance since it has been reported that DNA topology (supercoiled, open-circular, linear) may play a central role on the TE of lipid-plasmid complexes.[30]

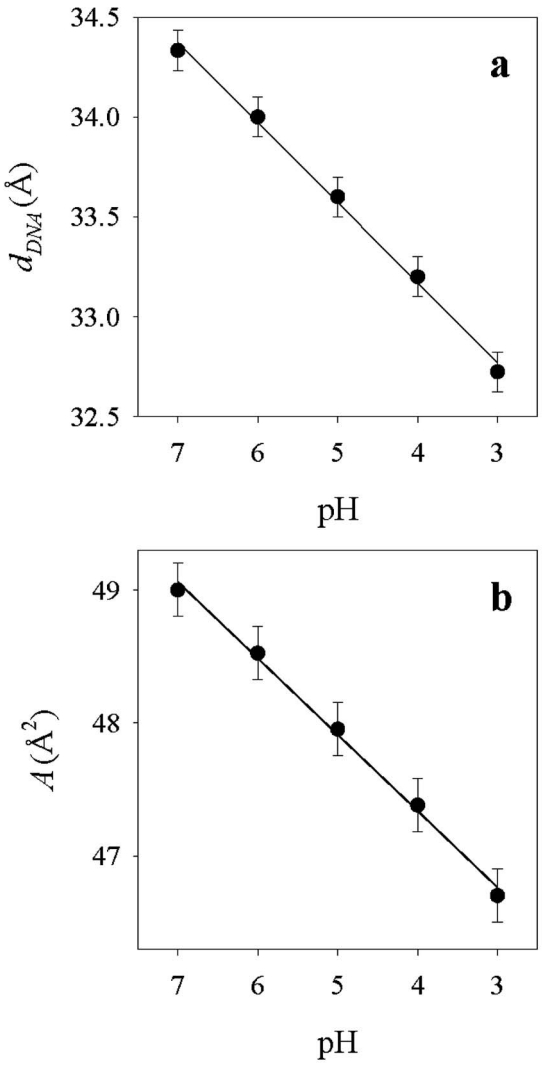

FIG. 4. Panel (a): DNA interdistance d_{DNA} as a function of *p*H for DC-Chol-DOPE/DNA lipoplexes. Panel (b): *p*H dependence of the average interfacial area A per lipid molecule of DC-Chol-DOPE membranes. Solid lines are the best linear fits to the data.

IV. DISCUSSION

The purpose of this work was to correlate the *p*H-induced structural changes in lipoplexes with the extent of DNA release and the TE.

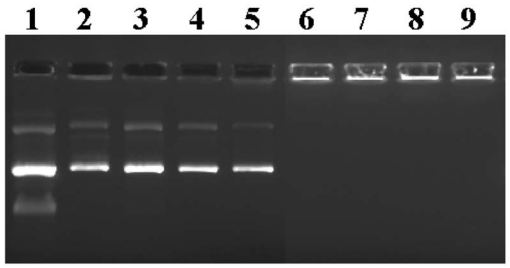

FIG. 5. Digital photograph of DOTAP-DOPC/DNA and DC-Chol-DOPE/DNA lipoplexes (ρ=2) at decreasing *p*H values. Lane 1: control DNA; lane 2: DOTAP-DOPC/DNA *p*H=7; lane 3: DOTAP-DOPC/DNA *p*H=5.5; lane 4: DOTAP-DOPC/DNA *p*H=4; lane 5: DOTAP-DOPC/DNA *p*H=3; lane 6: DC-Chol-DOPE/DNA *p*H=7; lane 7: DC-Chol-DOPE/DNA *p*H=5.5; lane 8: DC-Chol-DOPE/DNA *p*H=4; lane 9: DC-Chol-DOPE/DNA *p*H=3. In lane 1, the high-mobility band was attributed to the most compact (supercoiled) form, and the less-intense one was considered to be the nonsupercoil content in the plasmid preparation.

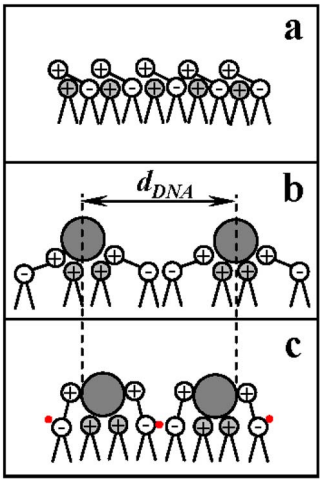

FIG. 6. (Color online) Schematic illustration of the proposed mechanism for the reduction in DNA spacings upon acidification. Panel (a): a mixed cationic-zwitterionic lipid membrane. The headgroup of the cationic lipid species carries one positive charge (gray circle). The headgroup of the zwitterionic lipid consists of a single dipole with spatially fixed negative-charge base and a mobile positive-charge head (white circle). Panel (b): mixing DNA and cationic liposomes results in the formation of locally ordered 1D arrays of DNA chains (dark gray circle) intercalated between charged membrane bilayers. The distance between DNA chains is indicated as d_{DNA}. Panel (c): upon lowering the *p*H, H_3O^+ molecules (red circle) form hydrogen bonding with P^- atomic groups. N^+ atomic groups align the headgroup dipole moment ($P \rightarrow N$ vector) against the dipole moment created by the H_3O^+ molecules. As a consequence, the interfacial area of lipid headgroups decreases and a lateral contraction of lipid bilayer occurs.

Endocytosis is the major pathway of entry of lipoplexes inside the cell, but the escape of DNA from endosomal compartments is thought to represent a critical obstacle. Recently, it has been proposed that successful DNA escape may be dependent on the possibility of lamellar lipoplexes to form fusogenic inverted hexagonal phase[21–24] induced by local *p*H lowering within endosomal compartments.[31]

SAXD experiments showed that, upon acidification, the lamellar structure of employed lipoplexes is essentially preserved with DNA remaining tightly bound to lipid bilayers and that no lamellar-hexagonal phase transition occurs. About the observed reduction in DNA repeat distance [Figs. 3 and 4, panel (a)], some hypotheses can be made. At the molecular level, low *p*H can cause the protonation of the headgroups of the zwitterionic lipids (both DOPC and DOPE molecules). In the case of neutral DOPC, the phosphate group, which is linked to the glycerol backbone, has a negative charge, while the choline group, which constitutes the free end of the headgroup, has a net positive charge. DOPE is identical to DOPC except that the choline headgroup is replaced by ethanolamine. Ethanolamine has a reduced attraction to water so fewer water molecules gather around the headgroup. This reduces the effective size of the headgroup compared to the hydrocarbon tails. For both lipids, P and N atoms preferentially lie in the plane of the membrane.[32] The spatial organization of the P^- and N^+ atomic groups allows pairs of DOPC (or DOPE) molecules to interact with each other via $P\cdots N$ and $N\cdots P$ double pairs [Fig. 6, panel (a)].

Mixing DNA and CLs results in the formation of locally ordered 1D arrays of DNA chains intercalated between charged membrane bilayers. The electrostatic attraction be-

tween cationic lipids and DNA charged molecules induces polarization of the positive charge carried by the lipid headgroups along the DNA helix axis [Fig. 6, panel (b)]. Upon lowering the *p*H, H_3O^+ molecules form hydrogen bonding with P^- atomic groups, thus creating a hydrogen bonding network between the PC (or PE) headgroups. As result, a positive potential in the bilayer interior (where *P* atoms are located) is produced. N^+ atomic groups may therefore protrude toward the interbilayer water region to align the headgroup dipole moment ($P \rightarrow N$ vector) against the dipole moment created by the H_3O^+ molecules. As a consequence of dipole moment alignment, the interfacial area of lipid headgroups decreases and a lateral contraction of lipid bilayers occurs [Fig. 6, panel (c)].[32] By simple geometric arguments, it is easy to suppose that the resulting lateral contraction of lipid bilayers forces the unreleased DNA molecules to get closer to each other.

By extrapolation, diffraction findings suggest therefore that there is no direct DNA release from lipoplexes simply associated with acidification. Such interpretation was confirmed by electrophoresis experiments showing that the amount of free DNA did not depend on the *p*H (Fig. 5). Thus, it was not possible to correlate variable TE with phase evolution of lipoplexes upon acidification and DNA release.

Conversely, electrophoresis experiments also showed that, at the same cationic lipid/DNA charge ratio ($\rho=2$), all the DNA is complexed by DC-Chol-DOPE liposomes, while less than 50% is protected by DOTAP-DOPC ones. The meaning of such results is that the cationic lipid/DNA charge ratio required to completely complex the DNA depends on the cationic lipid formulations used.

Comparing such findings with TE results reported in Fig. 1, we suggest that DNA-binding capacity of liposomes represents a significant barrier to efficient transfection. Indeed, DNA, unprotected by a coating of cationic lipid, is subject to rapid degradation by cytosolic DNase.

Since efficient transfection will require an optimal protection of DNA against degradation, it will not be enough to mix DNA and excess lipid to guarantee complete DNA complexation. Exact determination of the cationic lipid/DNA charge ratio required to completely complex the DNA will be an essential prerequisite to perform accurate transfection studies.

V. CONCLUSION

In the present study, we investigated the correlation between structural evolution of DOTAP-DOPC/DNA and DC-Chol-DOPE/DNA lipoplexes upon acidification, the extent of DNA release, and the efficiency in transfecting mouse fibroblast (NIH 3T3), ovarian (CHO), and tumoral myofibroblast-like A17 cell lines.

We have shown that, in all the cell lines, TE of DC-Chol-DOPE/DNA lipoplexes was about one order of magnitude higher than that of DOTAP-DOPC/DNA ones.

We have also shown that upon lowering the *p*H from physiological to acidic values (as those characteristic of endosomes), (i) the lamellar structure of DOTAP-DOPC/DNA and DC-Chol-DOPE/DNA lipoplexes was essentially preserved and that no lamellar-to-hexagonal phase transition occurred, (ii) the 1D DNA packing density within lamellar lipoplexes increased, probably reflecting a contraction of interfacial area of lipid headgroups, and (iii) DNA was not released from employed lipoplexes. Thus, our data suggest that acidification of lipoplexes within the endosomal compartment is not an obvious prerequisite in a model of a phase-mediated membrane destabilization.

Taken together, all our findings seem to suggest that parameters other than simple acidification determine the transfection capacity of a given complex. The present work strongly suggests that such interfering parameters may include the DNA-binding capacity of CLs, which in turn is governed by the chemical nature of the amphiphile. Optimization of cationic lipid/DNA complexes for transfection will require to determine the optimal cationic lipid/DNA charge ratio necessary to complex completely the DNA.

[1] P. L. Felgner, T. R. Gadek, M. Holm, R. Roman, H. W. Chan, M. Wenz, J. P. Northrop, G. M. Ringold, and M. Danielsen, Proc. Natl. Acad. Sci. U.S.A. **84**, 7413 (1987).
[2] P. L. Felgner, Sci. Am. **276**, 102 (1997).
[3] *Liposomes in Gene Delivery*, edited by D. D. Lasic (CRC, Boca Raton, FL, 1997).
[4] I. Koltover, T. Salditt, and C. R. Safinya, Biophys. J. **77**, 915 (1999).
[5] A. J. Lin, N. L. Slack, A. Ahmad, I. Koltover, C. X. George, C. E. Samuel, and C. R. Safinya, J. Drug Target. **8**, 13 (2000).
[6] G. Caracciolo, R. Caminiti, D. Pozzi, M. Friello, F. Boffi, and A. Congiu Castellano, Chem. Phys. Lett. **351**, 222 (2002).
[7] T. Salditt, I. Koltover, J. O. Rädler, and C. R. Safinya, Phys. Rev. Lett. **79**, 2582 (1997).
[8] T. Salditt, I. Koltover, J. O. Rädler, and C. R. Safinya, Phys. Rev. E **58**, 889 (1998).
[9] I. Koltover, T. Salditt, J. O. Rädler, and C. R. Safinya, Science **281**, 78 (1998).
[10] K. K. Ewert, H. M. Evans, A. Zidovska, N. F. Bouxsein, A. Amad, and C. R. Safinya, J. Am. Chem. Soc. **128**, 3998 (2006).
[11] J. J. McManus, J. O. Rädler, and K. A. Dawson, Langmuir **19**, 9630 (2003).
[12] J. J. McManus, J. O. Rädler, and K. A. Dawson, J. Phys. Chem. B **107**, 9869 (2003).
[13] J. J. McManus, J. O. Rädler, and K. A. Dawson, J. Am. Chem. Soc. **126**, 15966 (2004).
[14] G. Caracciolo, D. Pozzi, R. Caminiti, and A. Congiu Castellano, Eur. Phys. J. E **10**, 331 (2003).
[15] A. J. Lin, N. L. Slack, A. Ahmad, C. X. George, C. E. Samuel, and C. R. Safinya, Biophys. J. **84**, 3307 (2003).
[16] R. Koynova, L. Wang, and R. C. MacDonald, Proc. Natl. Acad. Sci. U.S.A. **103**, 14373 (2006).
[17] H. Ellens, D. P. Siegel, D. Alford, P. L. Yeagle, L. Boni, L. J. Lis, P. J. Quinn, and J. Bentz, Biochemistry **28**, 3692 (1989).
[18] D. P. Siegel and R. M. Epand, Biophys. J. **73**, 3089 (1997).
[19] S. Audouy and D. Hoekstra, Mol. Membr. Biol. **18**, 129 (2001).
[20] *Targeting of Drugs*, edited by G. Gregoriades and B. McCormack (Plenum, New York, 2000).
[21] B. Tycko and F. R. Maxfield, Cell **28**, 643 (1982).
[22] R. M. Straubinger, K. Hong, D. S. Friend, and D. Papahadjopoulos, Cell **32**, 1069 (1983).
[23] F. Labat-Moleur, A.-M. Steffan, C. Brisson, H. Perron, O. Feugeas, P. Furstenberger, F. Oberling, E. Brambilla, and J.-P. Behr, Gene Ther. **3**, 1010 (1996).
[24] I. M. Hafez, S. Ansell, and P. R. Cullis, Biophys. J. **79**, 1438 (2000).
[25] D. Pozzi, H. Amenitsch, R. Caminiti, and G. Caracciolo, Chem. Phys. Lett. **422**, 439 (2006).
[26] H. Amenitsch, M. Rappolt, M. Kriechbaum, H. Mio, P. Laggner, and S. Bernstorff, J. Synchrotron Radiat. **5**, 506 (1998).
[27] G. Cevc, Biochemistry **26**, 6305 (1987).
[28] A. E. Blaurock, Biochim. Biophys. Acta **650**, 167 (1982).
[29] G. Caracciolo, D. Pozzi, H. Amenitsch, and R. Caminiti, Langmuir **22**, 4267 (2006).

[30]J.-Y. Cherng, N. M. E. Chuurmans-Nieuwenbroek, W. Jiskoot, H. Talsma, N. J. Zuidam, W. E. Hennink, and D. J. A. Crommelin, J. Control. Release **60**, 343 (1999).
[31]P. C. Bell, M. Bergsma, I. P. Dolbnya, W. Bras, M. C. A. Stuart, A. E. Rowan, M. C. Feiters, and J. B. F. N. Engberts, J. Am. Chem. Soc. **125**, 1551 (2003).
[32]G. Caracciolo, D. Pozzi, and R. Caminiti, Appl. Phys. Lett. **90**, 183901 (2007).